



INTERNATIONAL ATOMIC ENERGY AGENCY
UNITED NATIONS EDUCATIONAL, SCIENTIFIC AND CULTURAL ORGANIZATION
INTERNATIONAL CENTRE FOR THEORETICAL PHYSICS
I.C.T.P., P.O. BOX 586, 34100 TRIESTE, ITALY, CABLE: CENTRATOM TRIESTE



H4-SMR 393/10

SPRING COLLEGE ON PLASMA PHYSICS

15 May - 9 June 1989

ALFVENIC TURBULENCE IN BEAM-PLASMA SYSTEMS (III)

A. Johnstone

Mullard Space Science Laboratory
University College London
Holmbury St. Mary
Surrey, RH5 6NT
Dorking
U. K.

PITCH ANGLE DIFFUSION

Gaffey et al JGR 93, 5470, 1988
 Gaffey & Wu JGR in press 1989

The equation for $\frac{\partial F}{\partial t}$ in quasilinear theory can be written as a diffusion equation in the wave frame

$$\frac{\partial F}{\partial t} = \frac{\partial}{\partial \mu} \left[(1-\mu^2) D \frac{\partial F}{\partial \mu} \right] + \epsilon S(v, \mu)$$

$$\mu = \cos \alpha \quad \epsilon = \frac{\partial n_i}{\partial t} \quad (\text{ionisation rate})$$

where

$$D = \frac{\pi q_e^2}{4 m^2 V_A^2} \int d^3 k I_k \delta(\omega - k v_0 \mu_0 - \Omega_i)$$

Assume $D(\mu) = D(\mu_0)$ to make problem tractable

$$\text{Put } F(\mu, v, 0) = \frac{n_i}{2\pi V_0^2} \delta(v - v_0) \delta(\mu - \mu_0)$$

PITCH ANGLE DIFFUSION SOLUTIONS

Gaffey, Wu JGR (in press), 1989

$$F(\mu, v, t) = \frac{1}{2\pi V_0^2} \delta(v - v_0) G(\mu, t)$$

$$G(\mu, t) = n_0 G_0(\mu, t) + \frac{\epsilon}{D} G_1(\mu, t)$$

$$G_0(\mu, t) = \sum_{l=0}^{\infty} (l+1) P_l(\mu) P_l(\mu_0) \exp[-D l(l+1)t]$$

$$G_1(\mu, t) = \frac{D t}{2} + \frac{1}{2} \sum_{l=1}^{\infty} \frac{(2l+1)}{(l+1)l} P_l(\mu) P_l(\mu_0) \left\{ 1 - \exp[-D l(l+1)t] \right\}$$

$$D = \frac{\pi}{2} \frac{\Omega_i^2}{B_0^2} \frac{V_A}{V_0} \frac{1}{|\cos \alpha|} P_B(\omega_\alpha)$$

$$\omega_\alpha = \Omega_i + k v_0 \cos \alpha$$

$P_B(\omega)$ - power spectral density of magnetic field at ω .

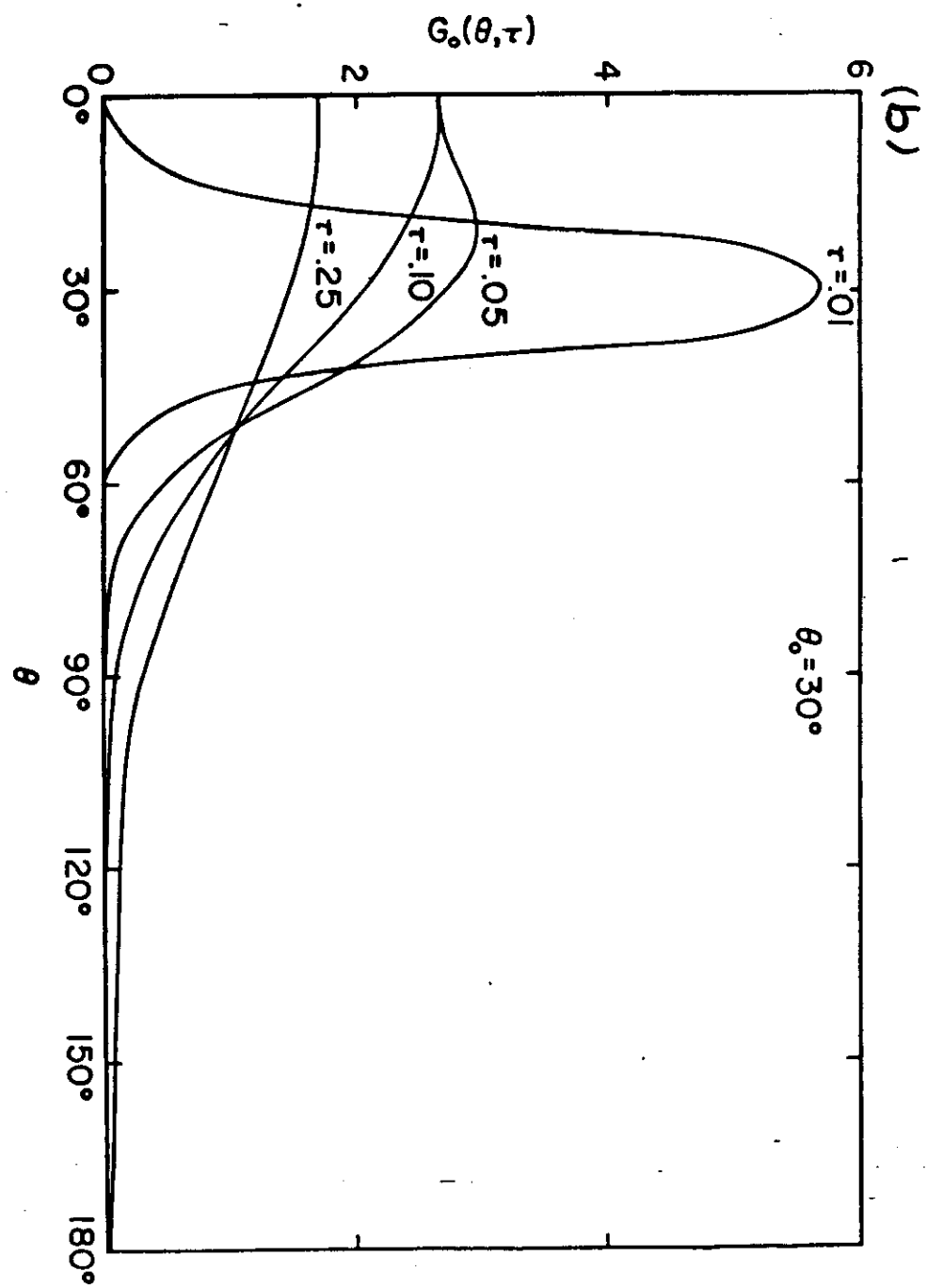


Figure 1b

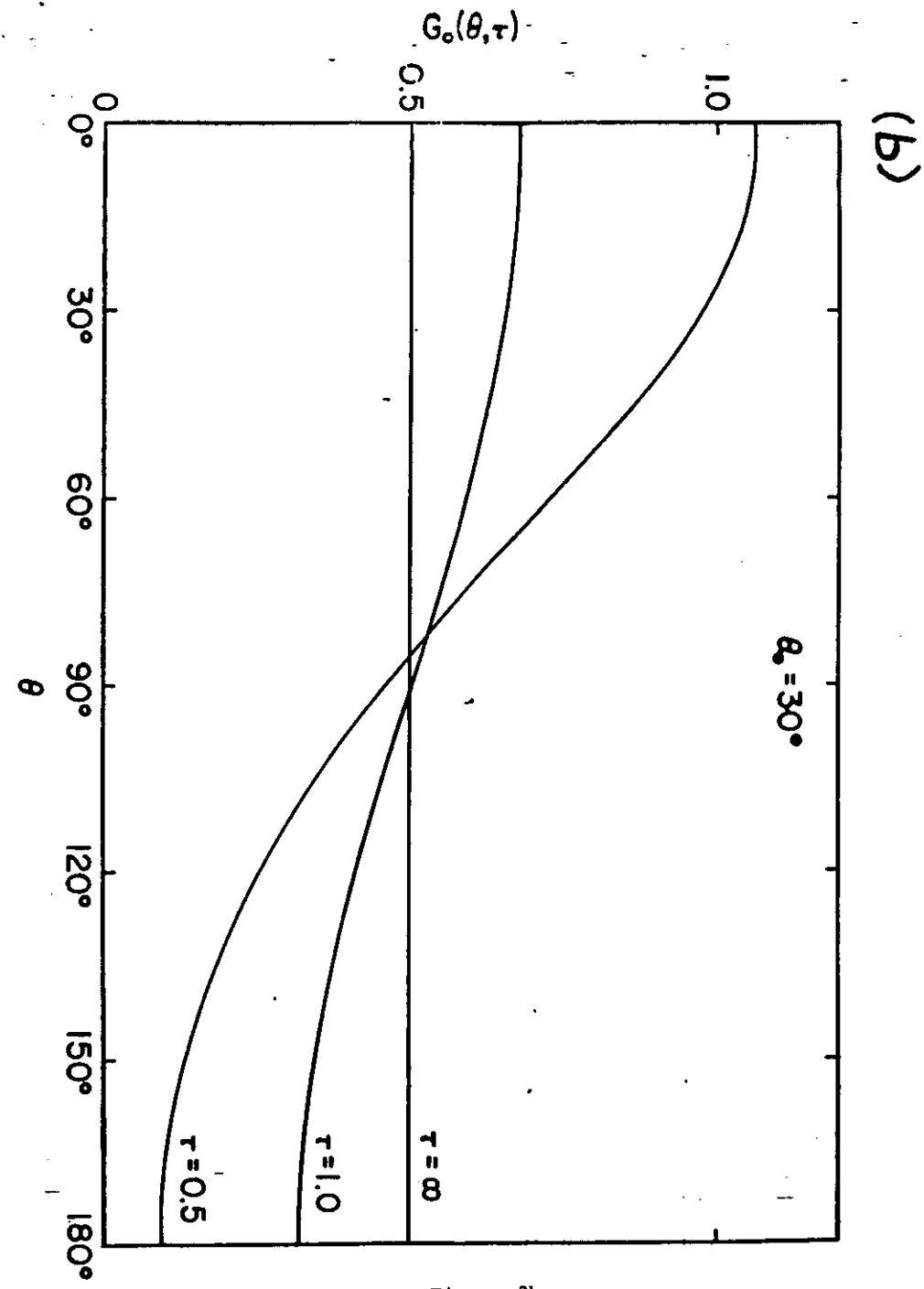


Figure 2b

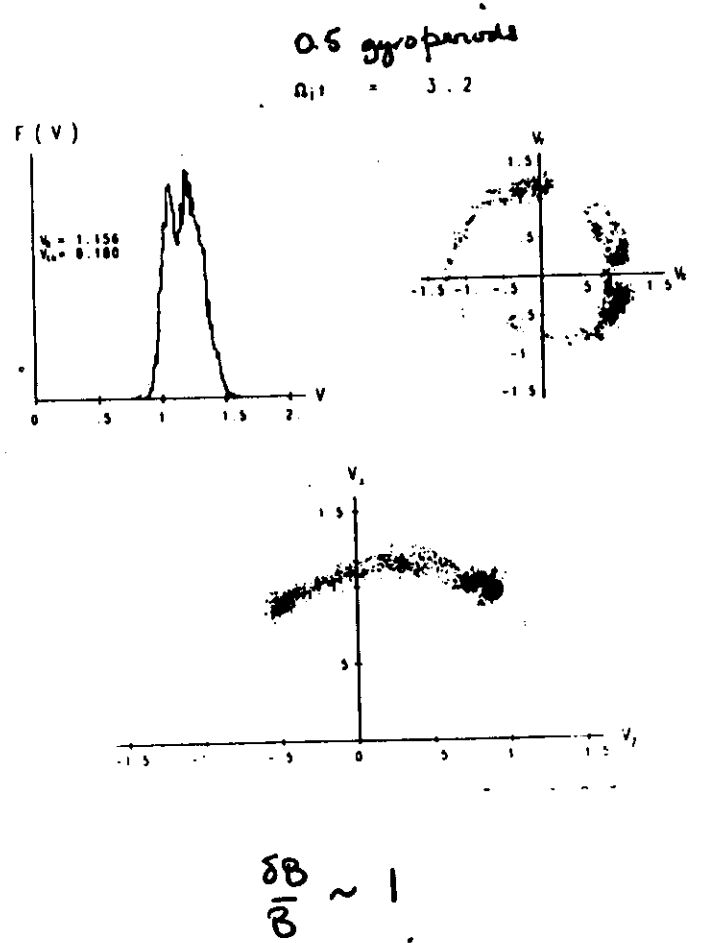
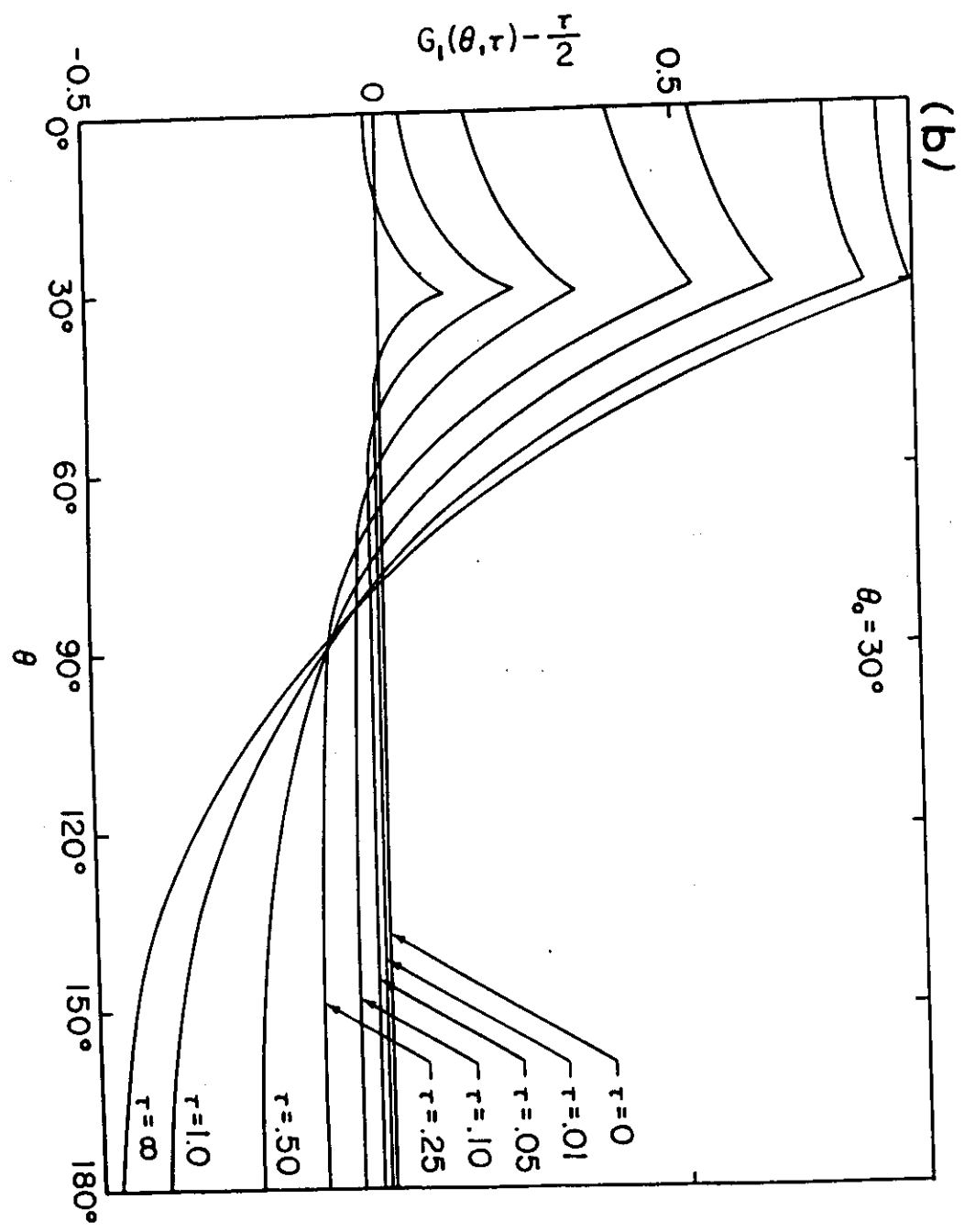


Figure 3b

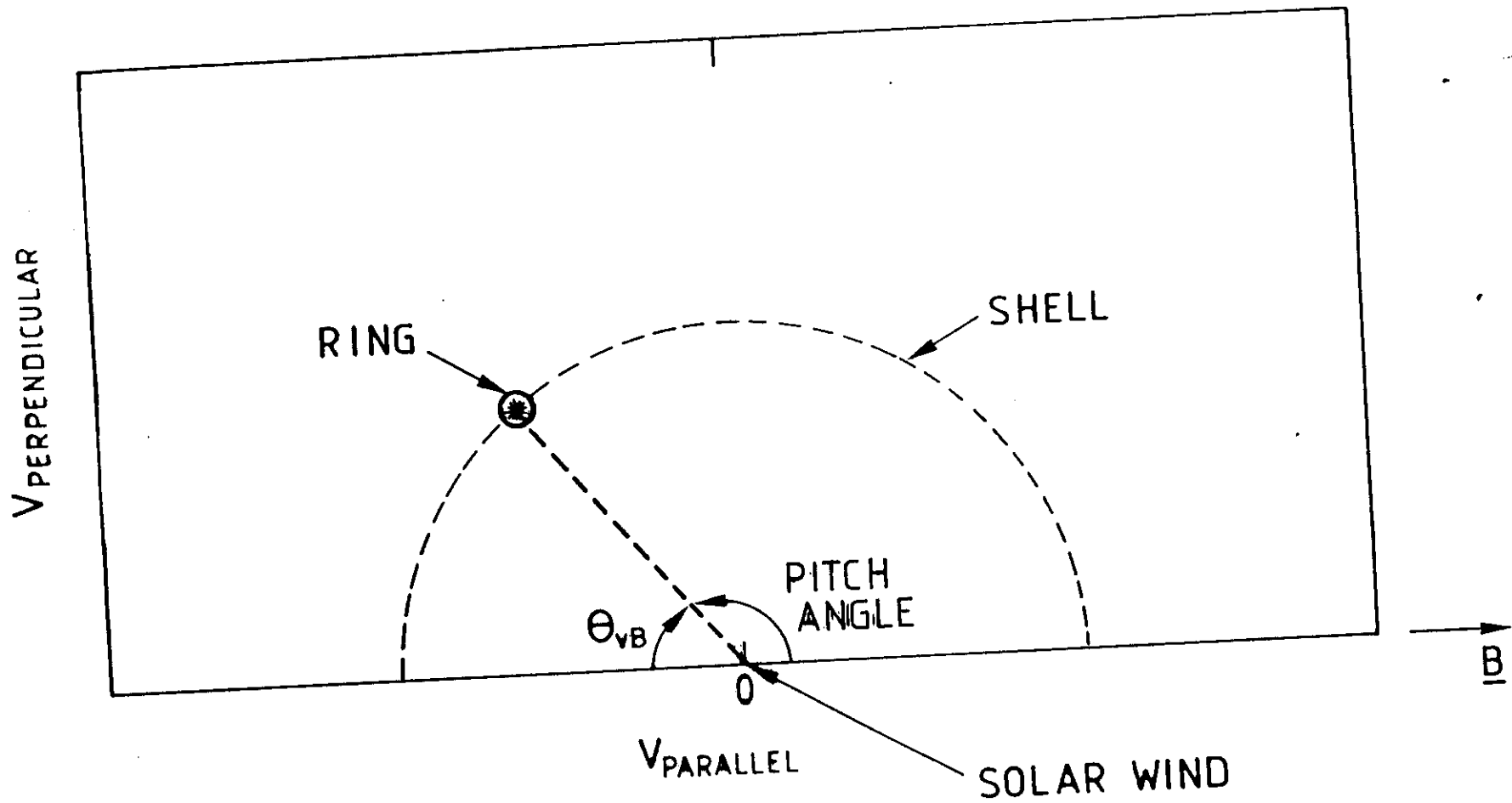


Figure 2 - View of the v_{\perp} - v_{\parallel} frame centred on the solar wind. Integration is performed in the gyro angle around \mathbf{B} . A ring distribution is marked by the circled star and a shell distribution centred on the solar wind speed is shown by the dashed semicircle. Figures 3-8 are data plots using this format.

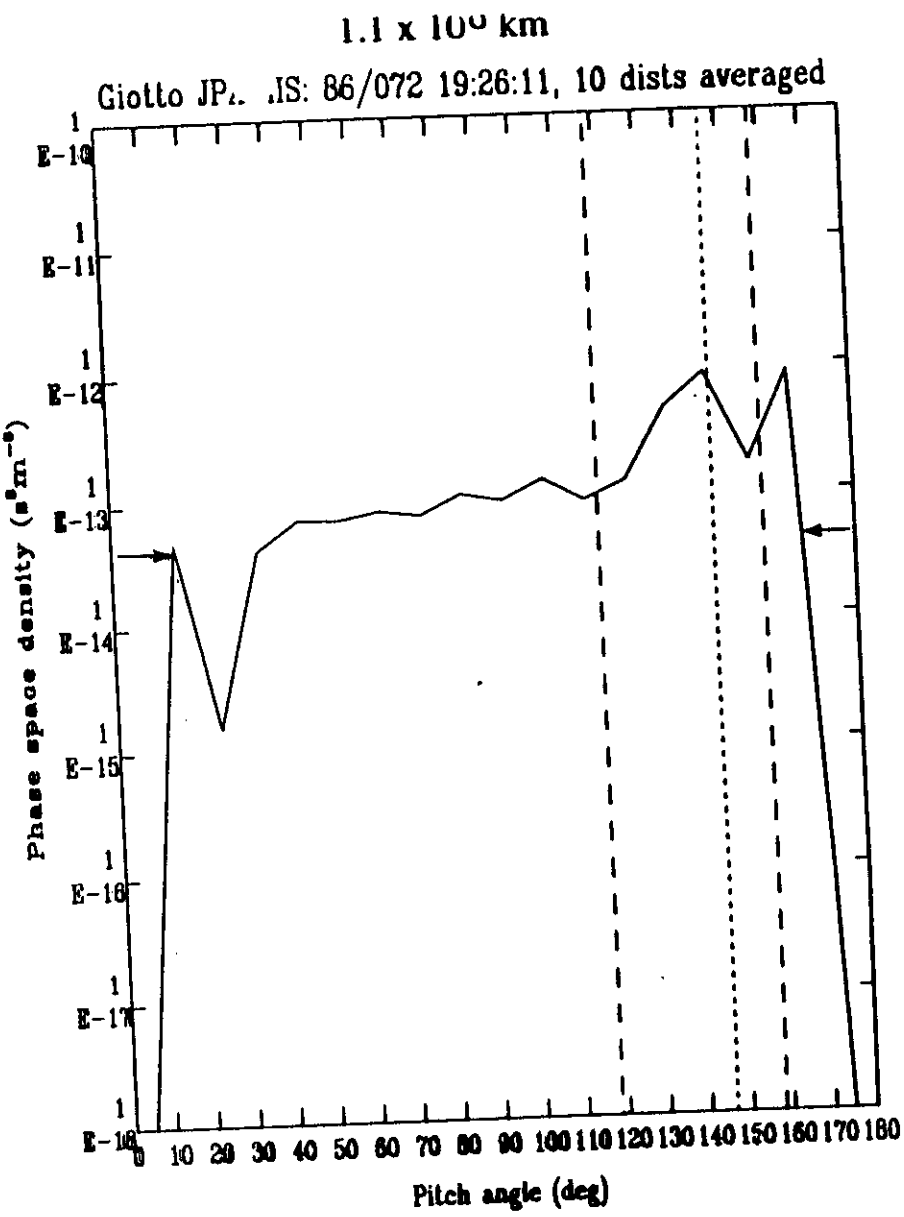
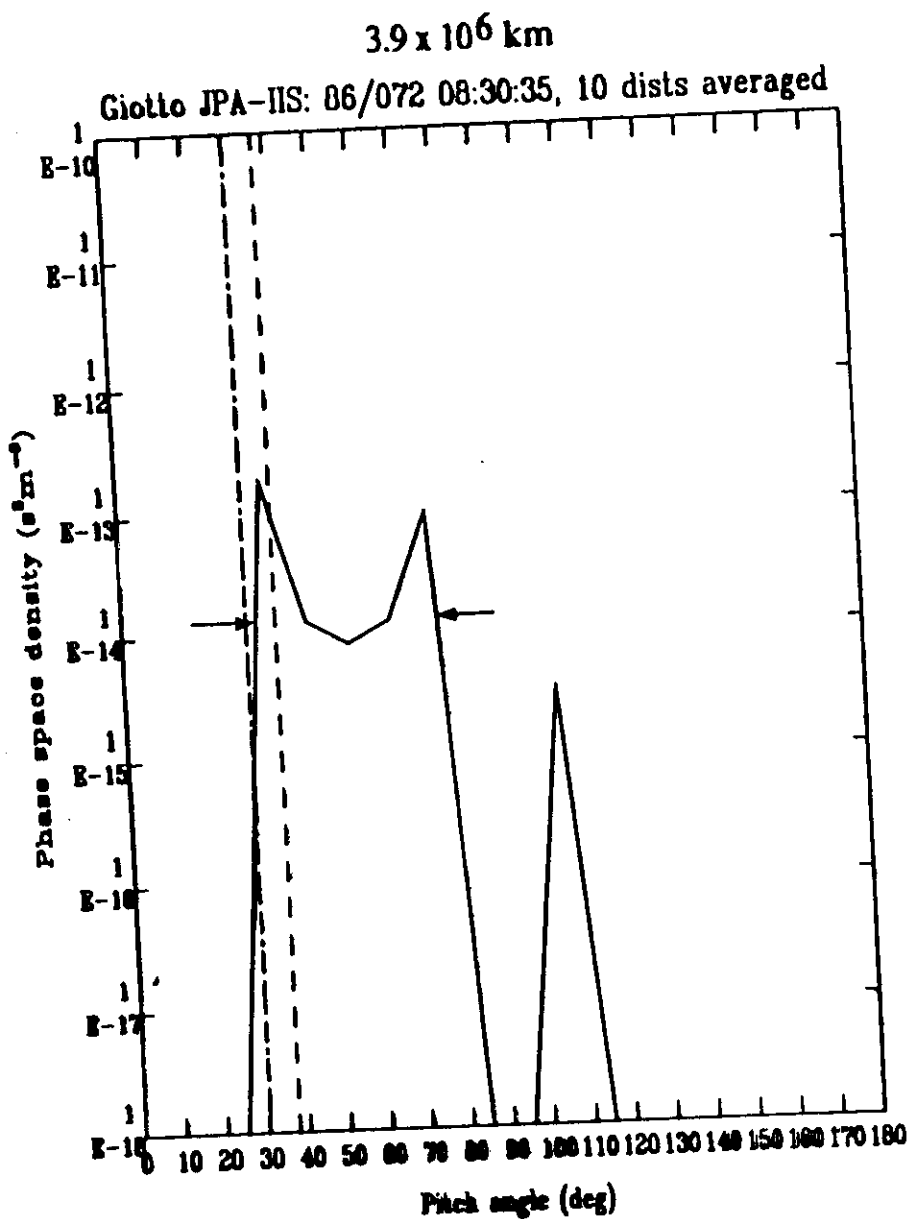


Figure 4 - Water group ion phase space density summed over energy as a function of pitch angle for two distances, (a) 3.9×10^6 km (b) 1.1×10^6 km. The pitch-angle width is defined as the width at 0.1 times the phase space density peak. There is some small filling in (b).

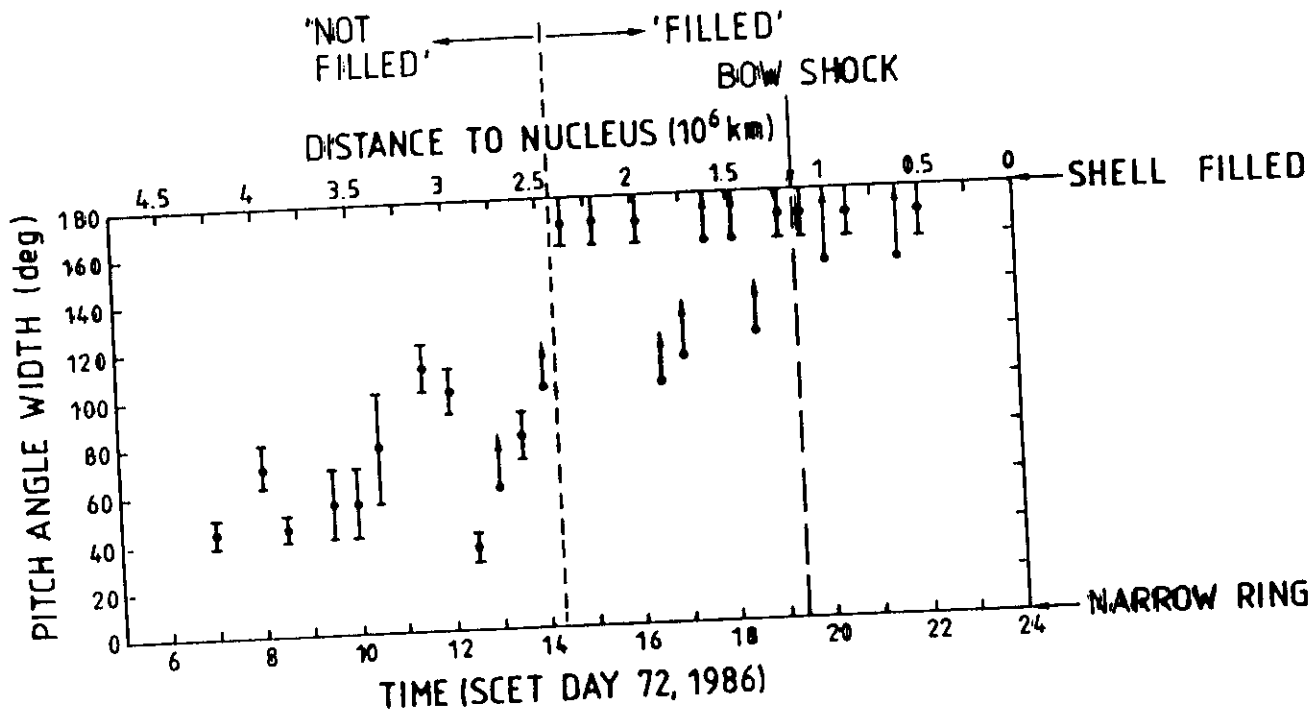
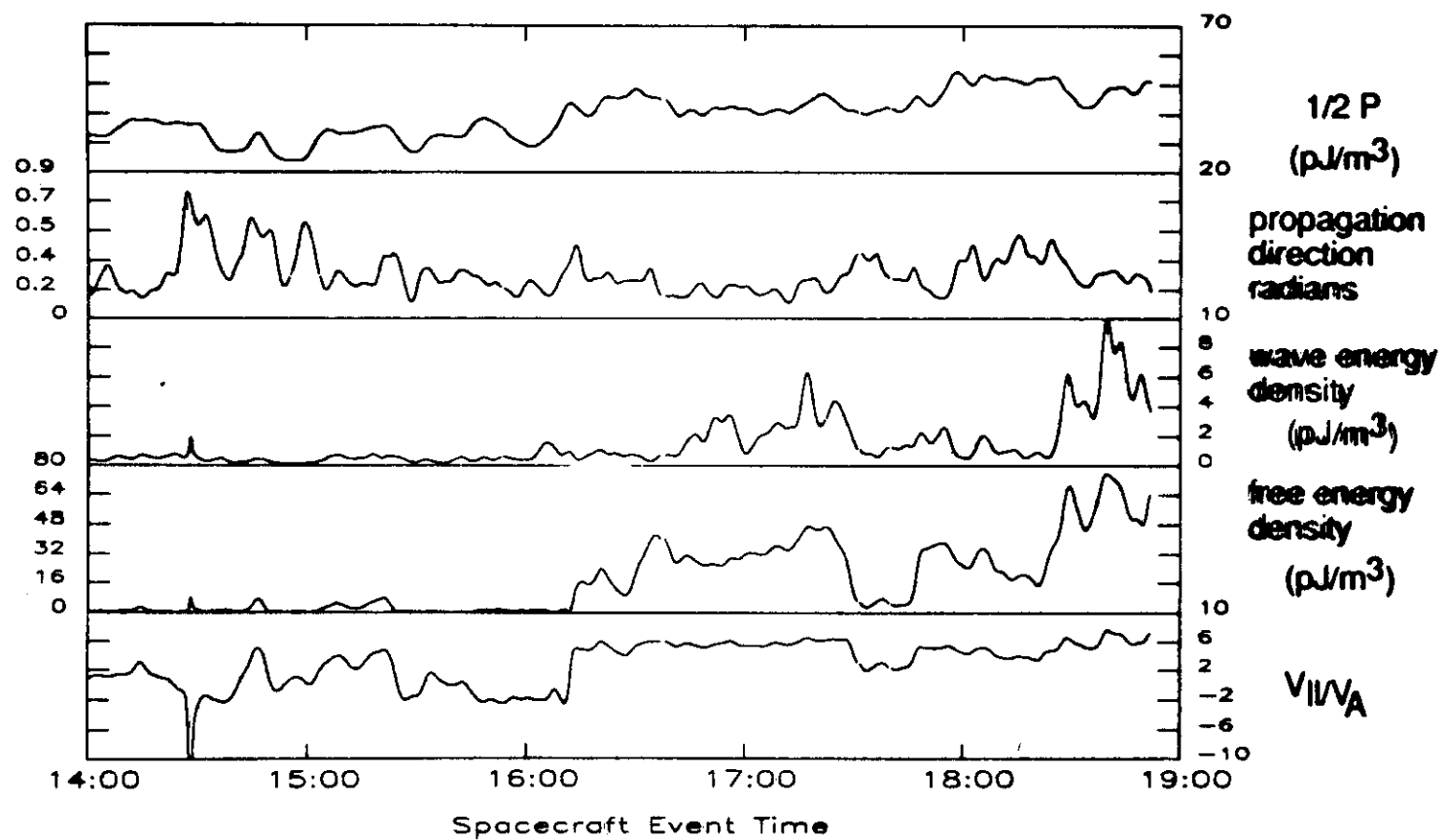


Figure 5 - Evolution of pitch-angle width with distance from the comet. A full shell would appear towards the top of the plot.

GIOTTO JPA FIS Solar Wind
Year 1986 Day 72



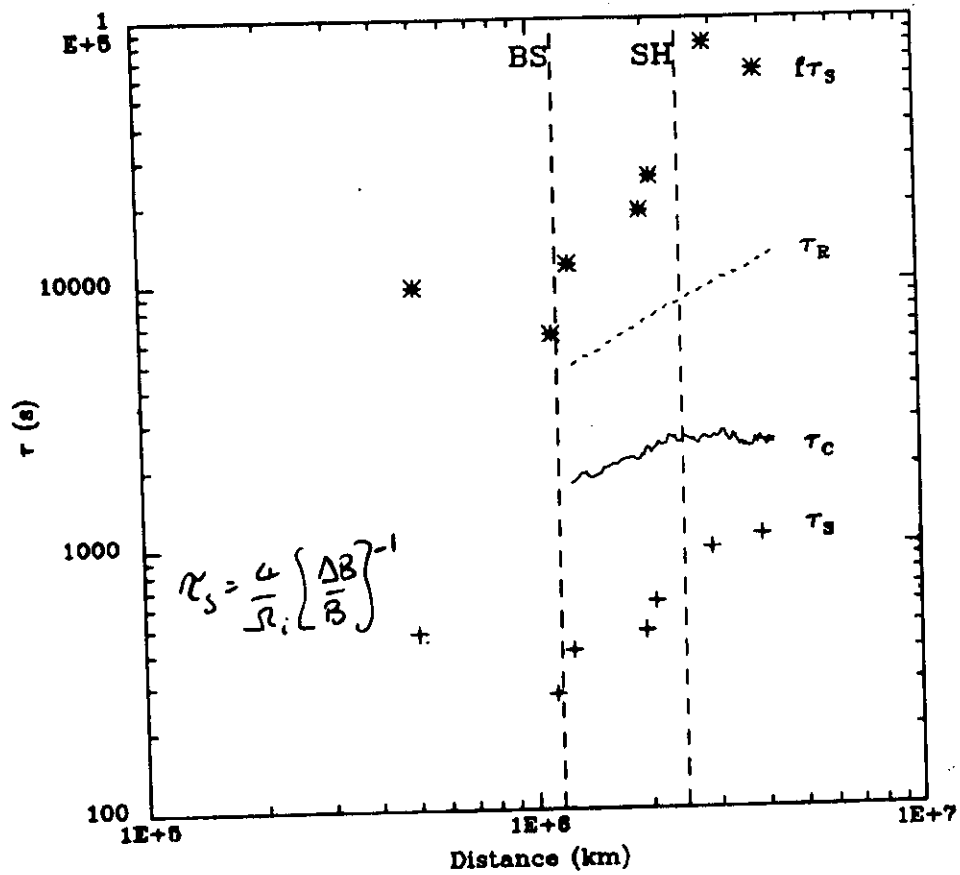


Figure 10 - Pickup times according to Equation 6 (r_A - pickup region size assuming constant ionization rate [Richardson et al, 1988]), Equation 7 (r_C - average time ions spend in solar wind flow [this paper]), Equation 3 (r_s - pitch angle scattering time [Gaffey et al, 1988]), and $f = (v_s/v_A)^2$ times r_s ($f r_s$ - energy scattering time [Lyons and Williams, 1984]). The vertical lines indicate the maximum distance where the observations show a filled shell (SH) and the position of the bow shock (BS).

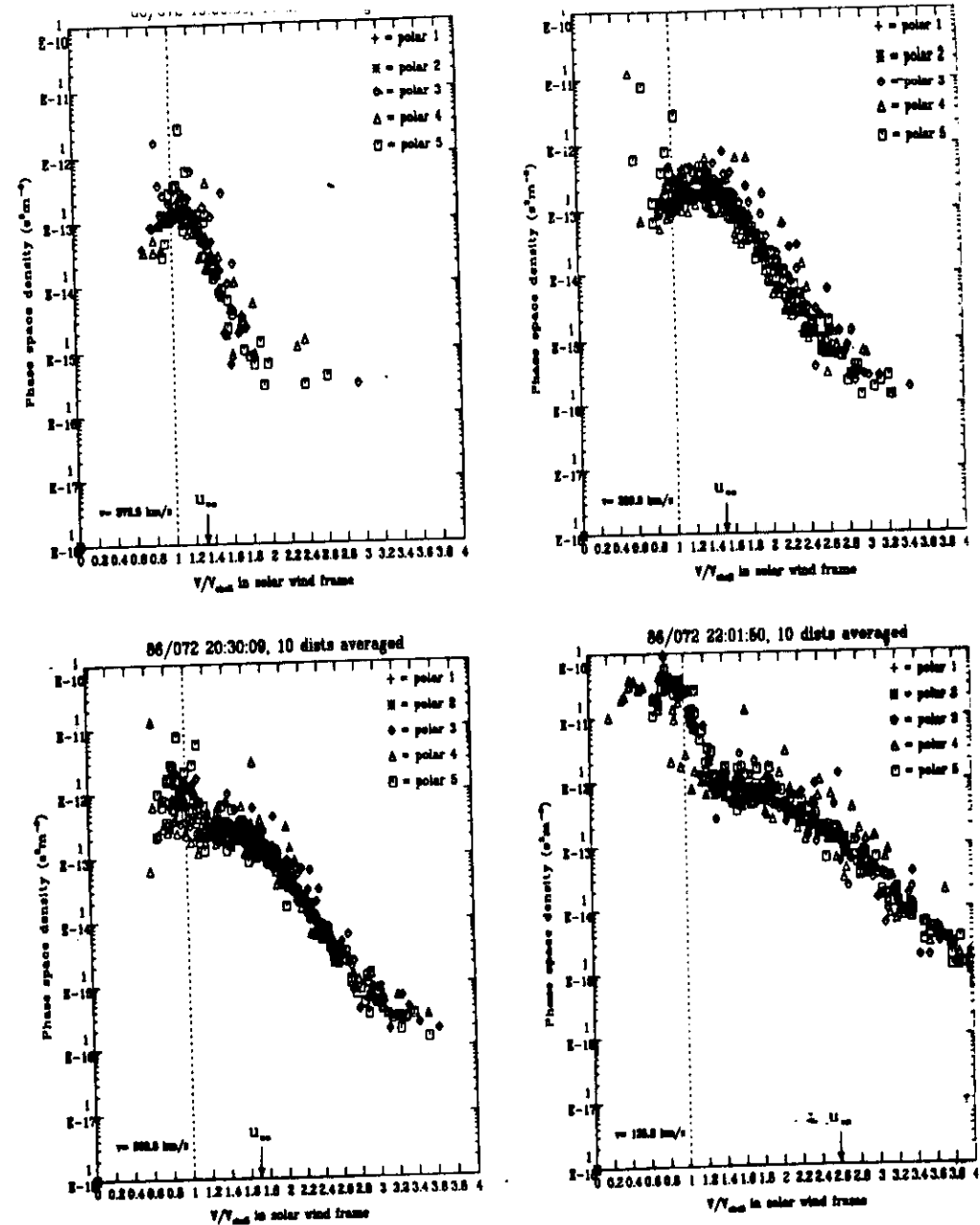
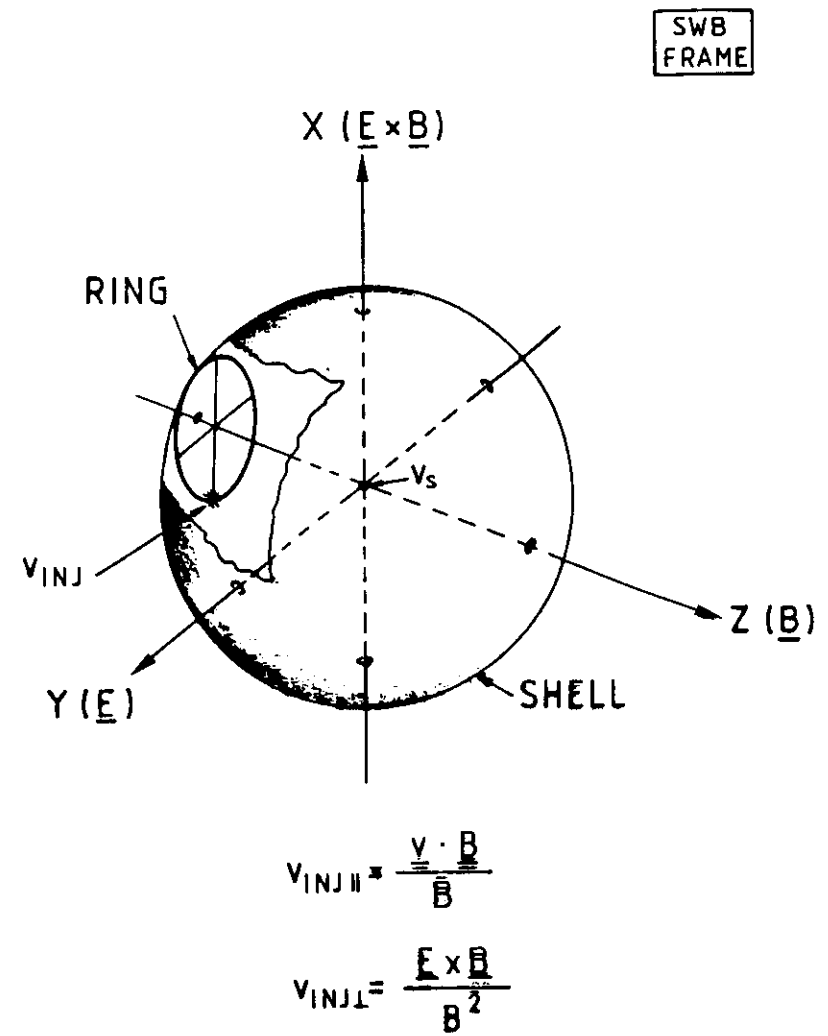


Figure 7 - Phase space density versus velocity normalised to the local solar wind speed, in the solar wind frame. Downstream of the shock a second component, travelling at the upstream solar wind speed (cf Thomsen et al 1987) is visible.



Predicted bulk velocities in SWB Frame

RING distribution $(0,0,v_{inj\parallel})$

SHELL distribution $(0,0,0)$

SHELL distribution,
centred on $\pm v_a$ along B $(0,0,\pm v_a)$

Figure 2 - The SWB (solar wind field-aligned) frame, showing the ion injection point (v_{inj} , shown by a star), ring and shell distributions, with the coordinates of v_{inj}

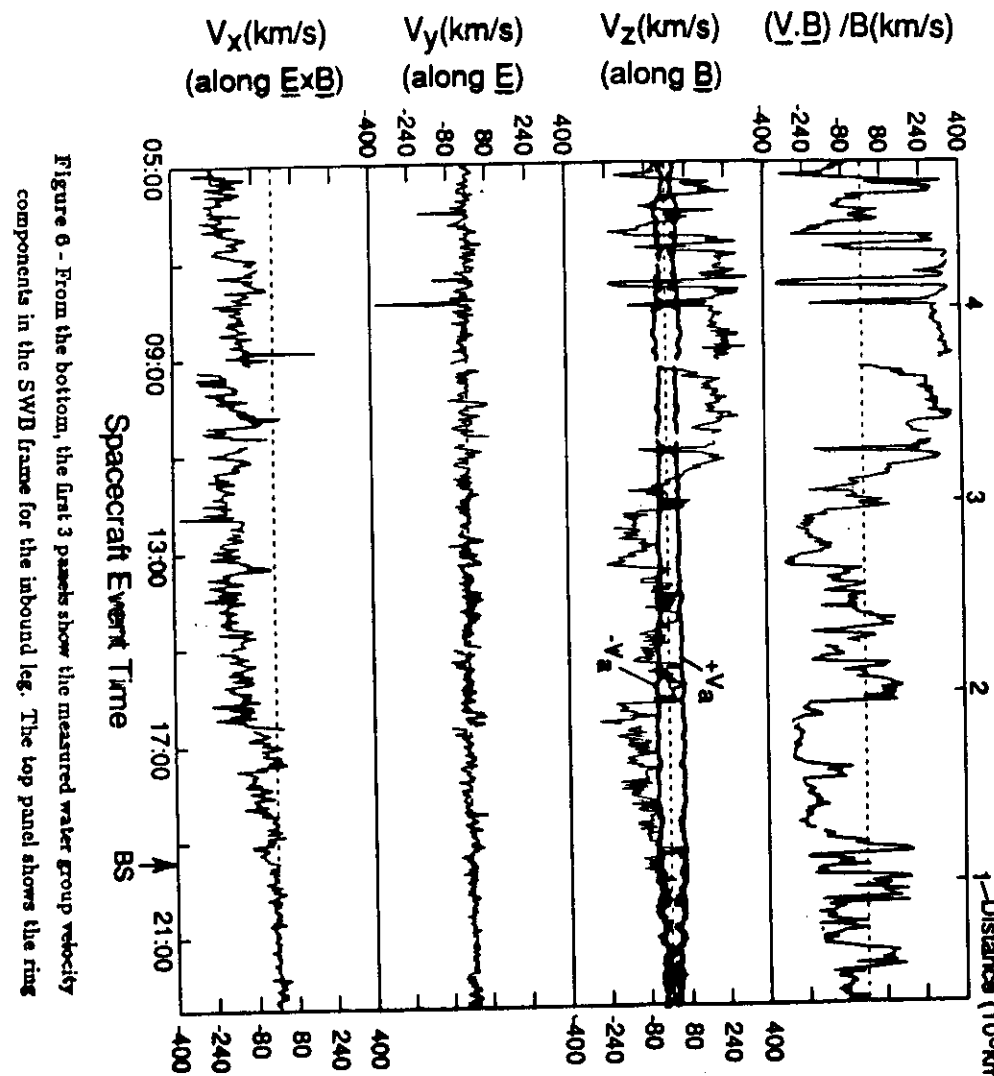
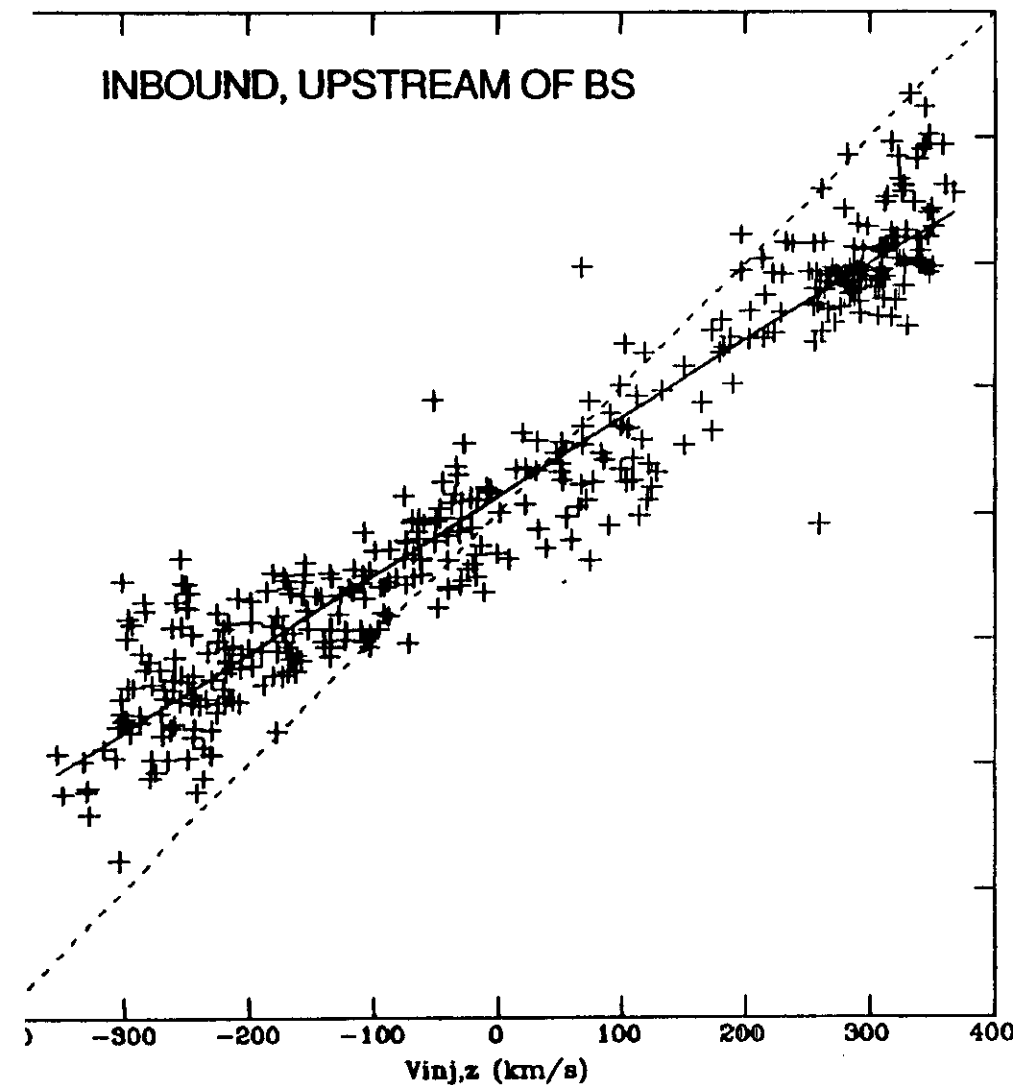


Figure 6 - From the bottom, the first 3 panels show the measured water group velocity components in the SWB frame for the inbound leg. The top panel shows the ring

Day 72 5: 0 to day 72 19: 0, slope=0.62, R=0.96



Day 72 19:30 to day 72 22:30, slope=0.10, R=0.43

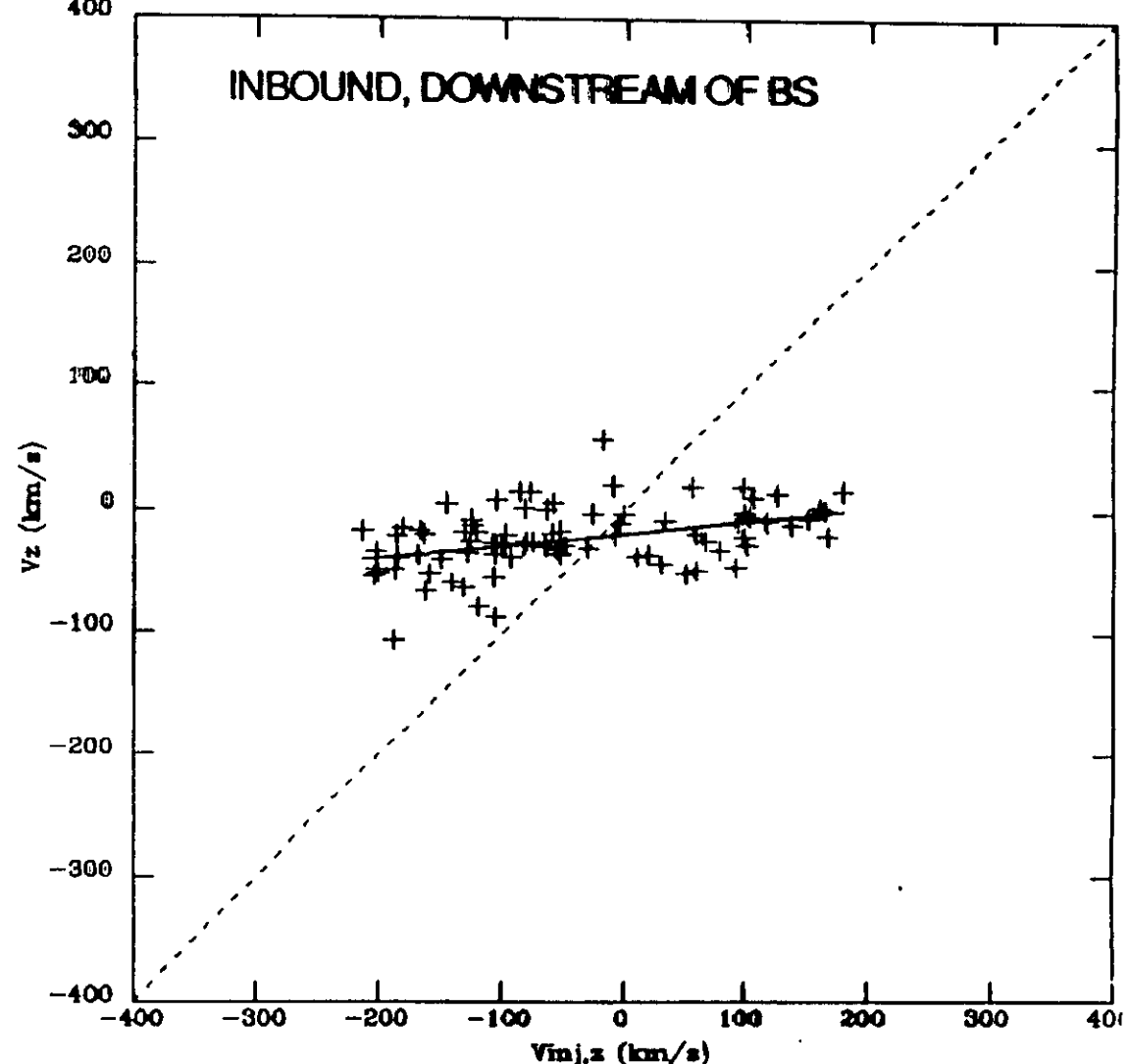


Figure 7 - (a) Scatter plot of the measured v_z component (ordinate) against the ring prediction (abscissa), upstream of the bow shock on the inbound pass. **(b)** Similar

G1-TTO JPA IIS oxygen bulk parameters
Year 1986 Day 73 SWB coordinates

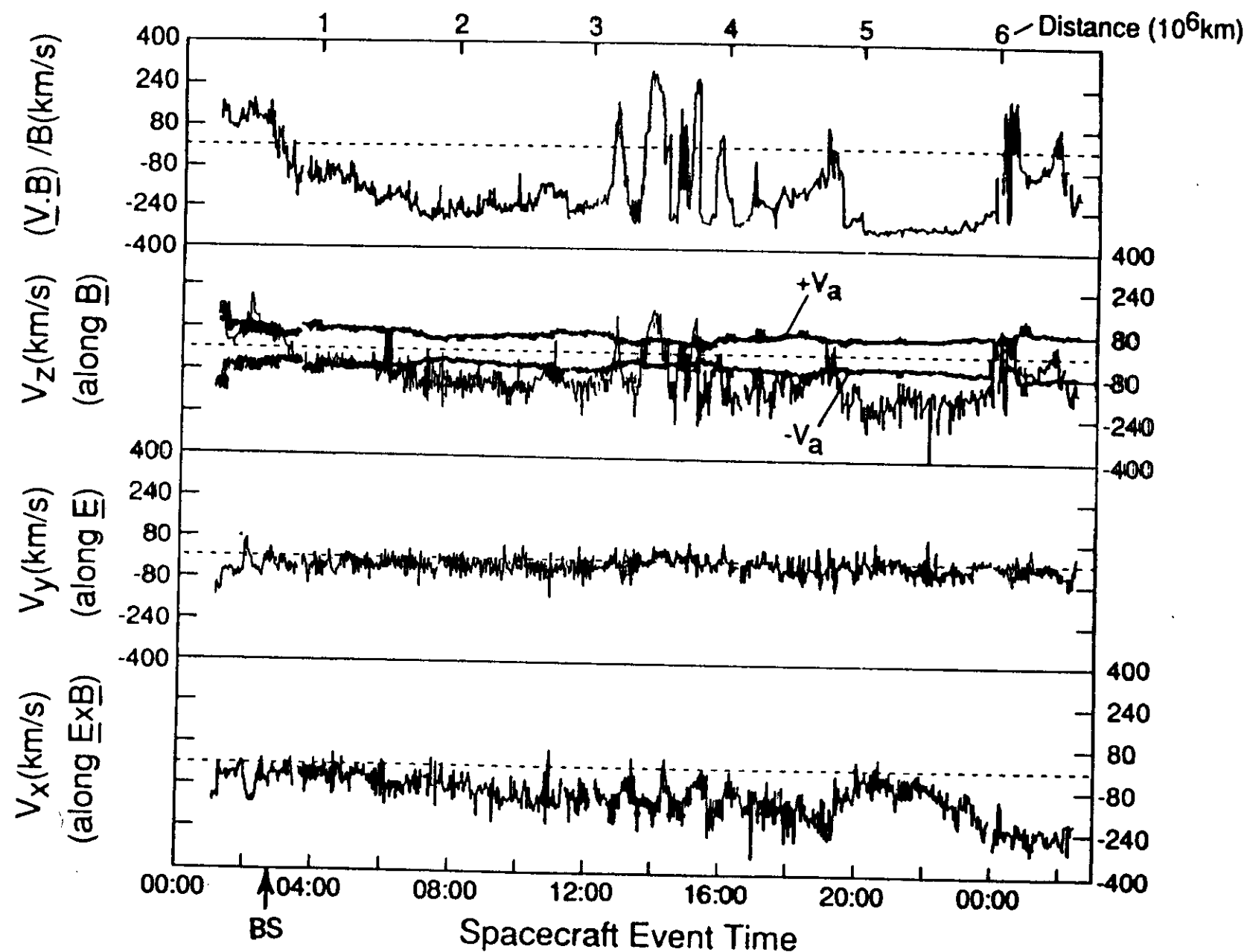


Figure 11 - From the letter ...

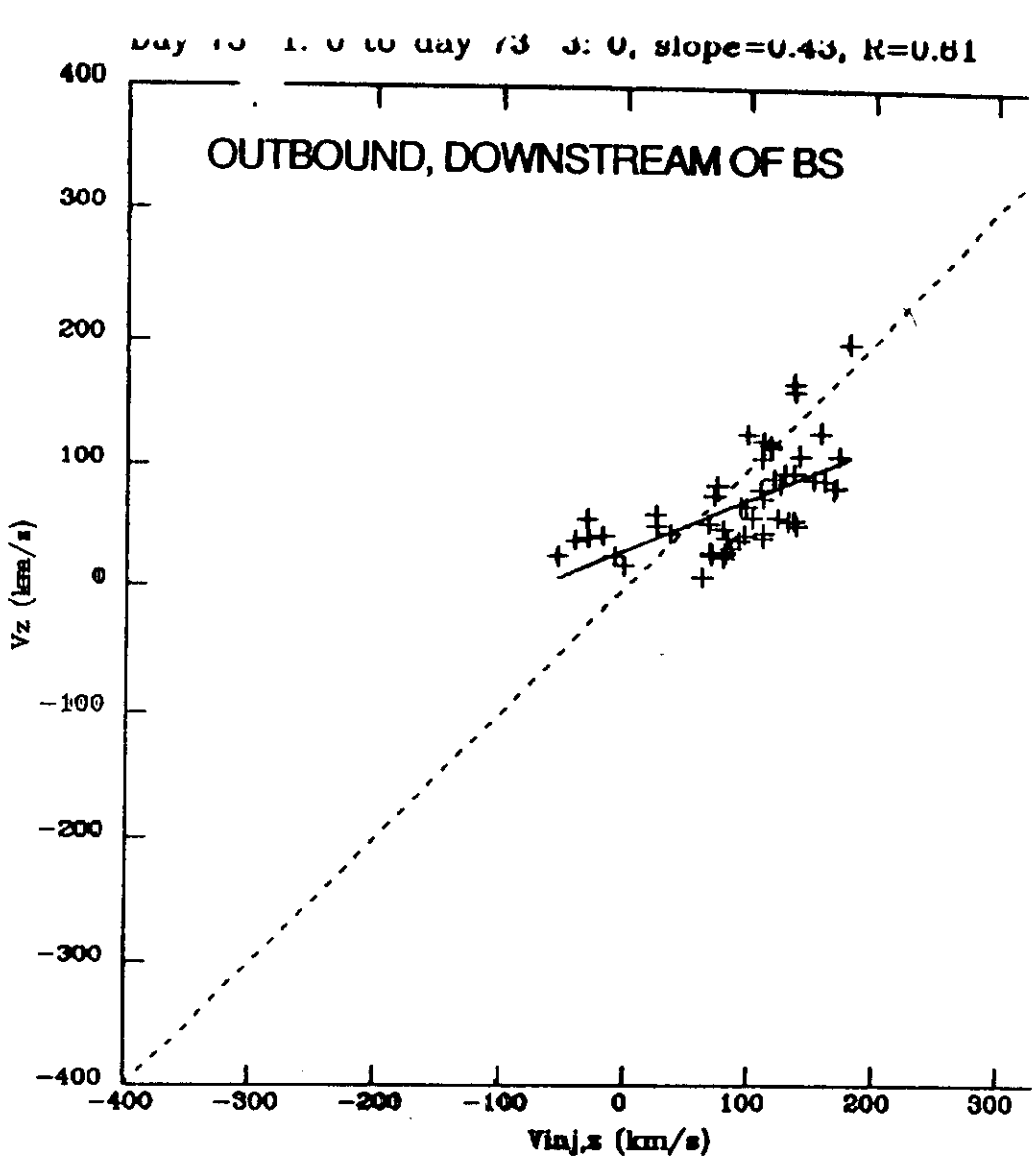
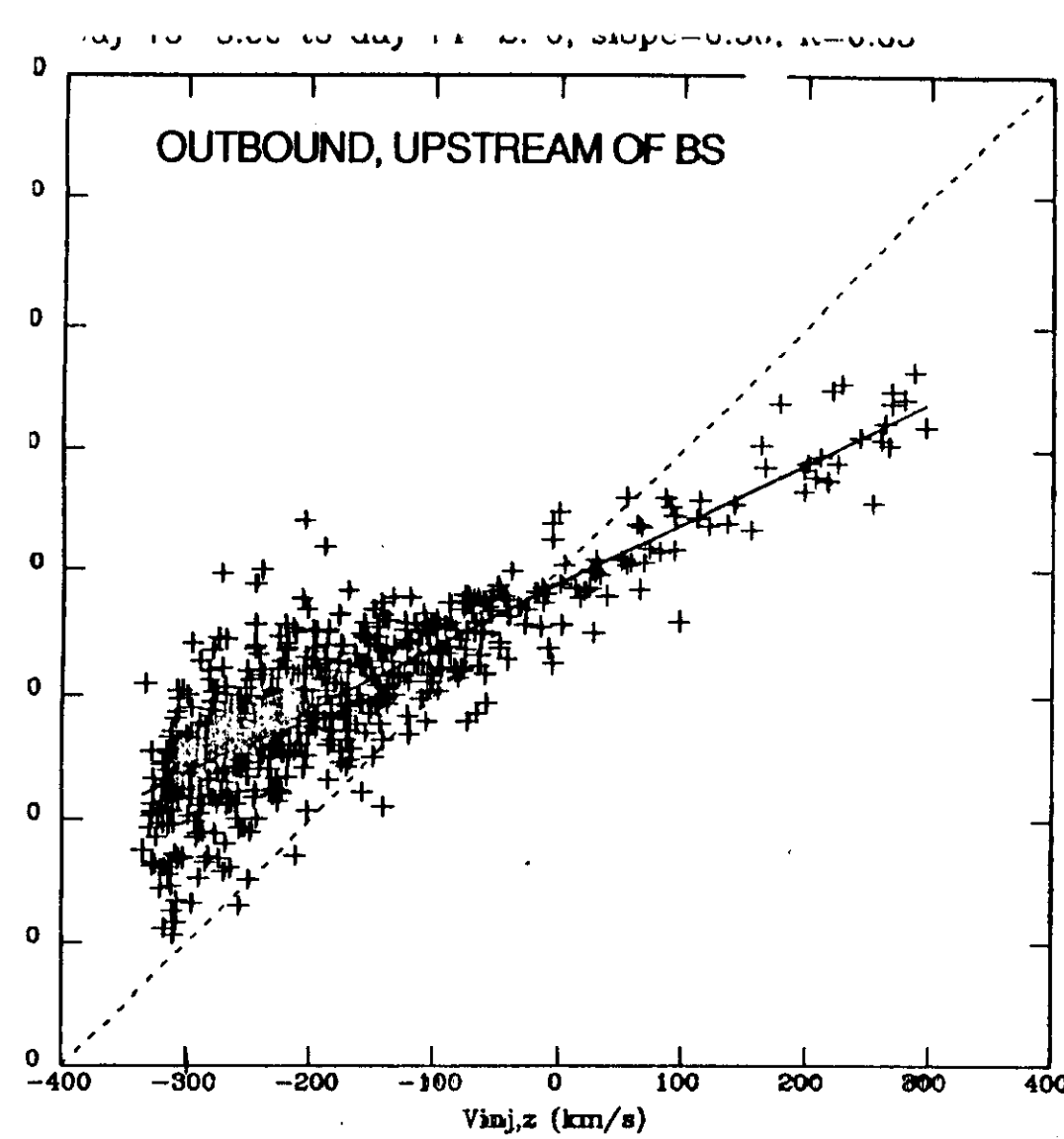


Figure 12 - (a) Scatter plot of the measured v_z component (ordinate) against the ring prediction (abscissa), upstream of the bow shock on the outbound pass. **(b)** Similar scatter plot for the downstream region.

